Direct ascent from air and N_2-O_2 saturation dives in humans: DCS risk and evidence of a threshold.

H.D. VAN LIEW AND E.T. FLYNN

Barnstable, MA 02630 and Naval Sea Systems Command, Washington Navy Yard, DC, 20376

Van Liew H.D., Flynn E.T. Direct ascent from air and N_2-O_2 saturation dives in humans: DCS risk and evidence of a threshold. Undersea Hyperb Med 2005; 32(6):409-419.To estimate the risk of decompression sickness (DCS) for direct ascents from depth to the sea surface for personnel who are saturated with hyperbaric nitrogen, we analyzed 586 experimental air or nitrogen-based saturation dives. No DCS occurred on shallow saturation dives between 12.0 and 20.5 feet of seawater, gauge (fswg) but incidence of DCS rose abruptly when depth was deeper than 20.5 fswg, reaching 27% at 30 fswg. This is evidence of a threshold for clinical DCS. A model based on a Hill function that provides for a threshold predicts the observations better than a model having no threshold provision; the no-threshold model overestimates risk shallower than 20.5 fswg and underestimates risk between 20.5 and 30 fswg. For situations such as submarine rescues, we recommend our threshold model when the exposure pressure is 33 fswg or less. We also discuss deeper dives where there are no human data; extrapolations can be quite different for models that provide for a threshold than for models that do not.

INTRODUCTION

If a dive qualifies as a "direct-ascent dive," also known as a "no-stop dive" or "no-decompression dive," a diver can have a low probability of being stricken with decompression sickness (DCS) if he ascends from the depth of the dive directly to the surface at a specified rate. If the bottom time at the depth of the dive is so long that the dive does not qualify for direct ascent, the diver can avoid DCS by spending time at "decompression stops" at various depths for times prescribed by a decompression table or by ascending slowly.

It is commonly assumed that a diver's body tissues come close to equilibrium with the inert gas of the breathing mixture when exposure to depth is a day or longer. Dives with such long bottom times are considered "saturation" dives, although 99% equilibration of all body tissues may actually take more than one day. Personnel in a disabled submarine may be subjected to elevated pressure for many days before they escape or are rescued (1,2). When a saturation dive does not qualify for direct ascent, the prescribed rate of decompression is very slow, 1 to 3 feet of seawater/hr (3). Saturated personnel may be able to ascend directly from shallow depths with a low risk of DCS but the DCS risk increases dramatically with increase of depth.

Information is scarce regarding the risks of direct ascents from saturation dives. The current U.S. Navy Diving Manual (3) allows a diver to make a no-stop ascent after unlimited duration at 20 feet of seawater, gauge (fswg; 1 fsw = 3.063 kPa; 1 meter of seawater, gauge = 3.266 fswg; 33.08 fswg = 2 atmospheres absolute). However, the manual does not provide guidance as to the risk of DCS if it is necessary to make a direct ascent from deeper saturation depths. For example, the manual allows a diver to make a no-stop ascent after exposure to 25 fswg for less than

10 hours, before he is saturated, but there is no information on the risk if the diver is saturated at 25 fswg and is forced to make a direct ascent.

The objective of this communication is to provide quantitative estimates of the probability of developing DCS (*Pdcs*) for no-stop ascents from saturation dives. For relatively safe shallow saturation dives, we develop predictive models from the limited data that are available. We also mention problems associated with extrapolating from relatively safe dives and of using high-risk animal dives (4,5) to augment datasets of human dives when estimating risks of no-stop ascents from saturation at deep depths where there are no human data.

We use a probabilistic approach in which a model is fitted to dive-outcome data by formal statistical methods, thereby tying model parameters to objective facts about dive outcomes and allowing estimation of the *Pdcs* for dive profiles (6,7). The older "deterministic" method was used to generate the U.S. Navy Standard Air Decompression Table (3) and most other decompression instructions in use today. The deterministic approach uses dive-outcome data in a less rigorous way – ascent criteria are adjusted in an *ad hoc* fashion until dive profiles are judged to be properly segregated into "safe" and "unsafe" categories.

METHODS

Calibration dataset.

In our calibration dataset, there are 111 rows, where a row is a listing for one or more divers who followed the same profile and had the same outcome (DCS or no DCS). Table 1 shows our calibration dataset sorted according to depth of the dive and the sources: publications and files from the U. S. Navy Decompression Database (8,9). For displays in graphs, we separated the data into 7 groups that had appreciable numbers of dives (left-hand column in Table 1). There are 448 dives and no DCS cases in the first five groups, 76% of the entire dataset. Total decompression times are in the column designated TDT. Values in the Cases Pred column are calculated from the results of the statistical fitting of the data for our probabilistic model called the "Thr20.5 Model."

A majority of the DCS-free dives listed in Table 1 are the shallow saturation dives performed at the Marine Resources Development Foundation, Key Largo, FL. A total of 362 sports SCUBA divers were saturated at one of several depths for 1-2 days, then decompressed to the surface (tidal variations of depth were $\pm$1 fswg or less). None of the sports divers developed DCS. Of the 362 dives, 111 dives are reported by Eckenhoff and coworkers (10); the other 251 dives are cited by Eckenhoff (11) as a personal communication from Monney and Olstad.

The sources identified by capitalized initials in Table 1 are from the U. S. Navy Decompression Database (8,9), which consists of a number of computer files, each representing a particular decompression study. Each of the Database files contains a series of sequential entries that provide information about persons who followed a given dive profile. Each profile entry bears a summary heading that describes key features of the profile (depth, bottom time, total decompression time, and number of subjects) and the observed outcome (DCS, marginal DCS, or no DCS). The summary heading is followed by a series of lines showing the depth/time nodes of the profile. In the U.S. Navy Database, we identified 224 single-level, direct-ascent dives with bottom times of one day or longer. Of the 224 dives, 159 are air-breathing dives (18 DCS cases). The remaining 65 dives (4 DCS cases) are from the ASATARE series; the breathing gas at depth was a nitrogen mixture with an inspired oxygen partial pressure of 0.4 bar which required

TABLE 1. SUMMARY OF DIVE PROFILES IN THE CALIBRATION DATASET

Group	Source/File	SubFile	Depth, (fswg)	Bottom time, min	TDT, min	Divers	DCS cases	Cases pred*
1	Eckenhoff (10)		12.0	2,880	Less than 5	25	0	0.0
2	Eckenhoff (10)		16.0	2,880	Less than 5	54	0	0.0
3	Monney (11)		17.0	1,440	?	188	0	0.0
4	Monney (11)		18.5	1,440	?	63	0	0.0
5	ASATARE **	Islander Dive 5	19.5	2,880	0.8	5	0	0.0
5	ASATARE **	Islander Dive 6	19.6	2,880	0.8	5	0	0.0
5	ASATARE **	Islander Dive 2	20.0	2,880	0.8	5	0	0.0
5	ASATNMR		20.0	5,767 – 6,180	10 - 14	16	0	0.0
5	NMR9209		20.0	4,284 - 4,313	7 - 12	30	0	0.0
5	ASATARE **	Islander Dive 13	20.1	2,880	0.8	5	0	0.0
5	ASATARE **	Islander Dive 7	20.2	2,875	0.8	5	0	0.0
5	ASATARE **	Islander Dive 12	20.2	2,862	0.8	5	0	0.0
5	Eckenhoff (10)		20.5	2,880	Less than 5	32	0	0.0
5	ASATARE **	Islander Dive 1	20.6	2,880	1.8	5	0	0.0
5	ASATARE **	Islander Dive 8	20.6	2,880	3	5	0	0.0
6	NMR9209		22.0	4,298 – 4,400	7	12	0	0.3
6	ASATFR	7 msw Dive	22.8	2,160	2	3	0	0.2
6	NMR9209		23.3	4,303	12	6	2	0.4
6	ASATARE **	Islander Dive 4	23.5	2,880	2	5	1	0.3
6	ASATARE **	Islander Dive 11	23.9	2,880	2	5	1	0.4
6	ASATNMR		24.0	4,320	0.4	18	1	1.6
6	ASATARE **	Islander Dive 3	24.1	2,880	1.4	5	1	0.4
6	ASATARE **	Islander Dive 10	24.2	2,880	3	5	1	0.5
6	ASATARE **	Islander Dive 9	24.5	2,882	5	5	0	0.5
6	ASATTNSM	Minisat 1	25.5	2,880	1.3	19	0	2.6
6	ASATFR	8 msw Dive	26.1	2,160	2	3	0	0.5
6	ASATDC		26.4	1,440	1 - 3	14	2	2.3
7	ASATFR	9 msw Dive	29.4	2,160	2	1	0	0.3
7	ASATTNSM	Minisat 2	29.5	2,880	1.4	15	4	3.9
7	ASATDC		33.0	1,440 – 2,160	1	9	6	3.2
7	EDUAS45		33.0	1,440	2	12	2	4.2
7	NEDU correspondence		38.0	1,440	1.5	1	1	0.5
Totals						586	22	22.0 ± 7.9***

* estimates by the Thr20.5 Model

** depth is equivalent air depth, breathing gas is 0.4 bar O_2 in N_2

*** 95% confidence interval of the prediction

calculation of an equivalent-air depth.

We carefully studied the details of the time and depth profiles for each dive. Most of the dive profiles listed a single value for dive depth. No doubt there were small variations around this mean depth during the course of the exposure not captured in the Database. From our experience we judge that this variation is less than ± 1 fswg. During the ASATNMR exposures, 32 DCS-free subjects at a dry saturation depth of 20 fswg made one or more wet excursion dives to 22-23 fswg that lasted from 10 to 373 min; we excluded 16 of the subjects who had post-excursion intervals between 3 and 8 hr before final decompression to the surface; the included subjects had post-

excursion intervals of 26-31 hour at 20 fswg.

We applied corrections to the published information for three of the files from the Database: a) for the NMR9209 file we increased the dive depth from 22.0 to 23.3 fswg for 6 of the 18 subjects based on a review of the dive logs and supporting documentation that showed a depth-keeping error; two of these six subjects suffered DCS, b) we recalculated the equivalent-air depth for the ASATARE (Islander) series, using the recorded partial pressure of N_2 during the dive rather than the dive depth, and c) for the ASATFR85 file we changed the numbers of divers from 6 to 3 at depths of 7 and 8 meters of seawater based on a personal communication with the investigator (G. Masurel, 11 Feb 2003).

We wanted to make inferences only about DCS cases that would require active treatment so when cases in the Database are designated as "marginal" (defined as signs or symptoms that are diagnosed as DCS but not severe enough to require treatment), we assigned them as non-cases. Marginal cases have the same bottom times and depths as DCS cases, with one exception: a dive to 25 fswg for 2 days.

Data that are included in the U.S. Navy Decompression Database have been carefully scrutinized and screened for accuracy (8,9). The dives from the works of Eckenhoff et al. (10,11) have not been subjected to this same screening process but we do not see any reason to doubt the depth measurements or findings of zero DCS cases in these shallow dives.

The average total decompression time for the dives in our saturation dataset for which information is available is 6 min, with maximum of 14 min. We assume that the tissues that are susceptible to DCS after saturation dives release excess gas slowly so no-stop ascents slower than the 30 fsw/min mandated by diving tables for conventional no-stop diving will not bias our results unduly.

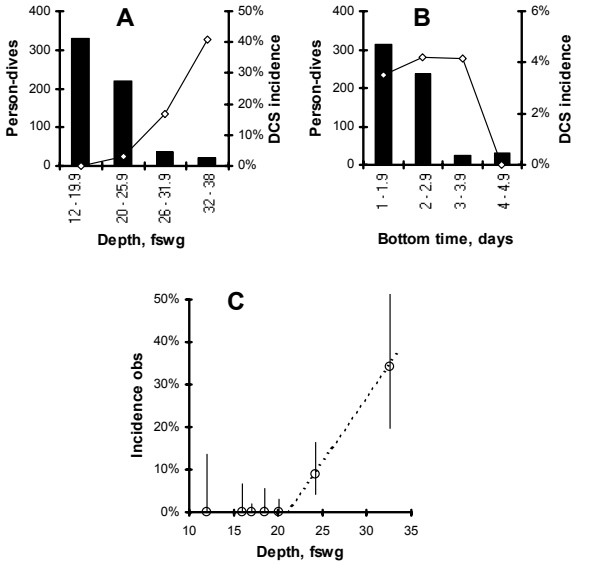

Fig. 1. Distributions of variables in the calibration dataset. A: distribution as a function of depth (or equivalent-air depth for dives in which an N_2-O_2 mixture was breathed); height of columns show total dives, line trace shows incidence of DCS. B: distribution as a function of bottom time. C: circles show observed incidence vs. depth or equivalent-air depth in groups of divers; vertical line segments show binomial 95% confidence intervals for the data points; straight dotted line is to lead the eye.

The bars in Figure 1A show there are few exposures deeper than 26 fswg; the line trace shows the incidence of DCS reaches 40% for the 32 to 38 fswg category. The bars in Figure 1B show the majority of the dives have bottom times of 3 days or less and the line trace shows that the incidence is about 4% for dives between 1 and 3.9 days duration. Incidence is zero for the longest dives; the dives with bottom times of 4 or more days are all at shallow depths.

The data we have assembled show that the incidence of DCS is zero for direct ascent from saturation depths shallower than a certain cutoff depth; that is, there is a threshold depth for DCS in saturation no-stop dives. Thus the dataset is made up of two populations. The dose-response relationship in Figure 1C is a plot of the DCS incidence in each of the 7 data groups (left-hand column in Table 1) versus

average depth in the group. The 95% confidence interval for 20.2 fswg in Figure 1C is from zero to 3.1% *Pdcs* and the lowest confidence interval is from zero to 1.9% at 17 fswg. The dotted line has a slope of about 3% per foot of seawater. There are 22 DCS cases among 586 dives in our calibration dataset, so overall DCS incidence is 3.75%. All the cases occur among the 180 dives that are 20.5 fswg or deeper so incidence among dives that are at the threshold or deeper is 12%. In deeper dives, some divers suffered neurological symptoms but in shallow dives, the DCS cases were limb bends so the threshold we estimate is the threshold for limb bends. It is important to note that Eckenhoff et al. (10,11) observed venous gas emboli in some subjects after ascent from all saturation depths between 12 and 20.5 fswg. Thus, at least to depths as shallow as 12 fswg, there is no threshold for venous gas emboli.

Probabilistic models with and without threshold.

We use the NONLIN module of a commercial statistical program, SYSTAT, with a Hill function that provides for a threshold:

$$1) \quad P_{dcs} = \frac{(D - Thr)^n}{(D - Thr)^n + (D_{50} - Thr)^n}$$

In Equation 1, D is depth or equivalent-air depth in fswg, *Thr* is threshold depth in fswg, n is the Hill-equation exponent, and D_{50} is the depth at which the *Pdcs* is 0.5, or 50%. Bottom time is not a relevant variable when a person's tissues are saturated. We use a Hill function because it is a well-known dose-response relationship, but the fundamental nature of DCS may be such that the data would be more accurately represented by some other relationship.

The discontinuity that is inherent in a threshold presents a problem. Because the dataset consists of two populations, it follows that the above-threshold and below-threshold dives should not be combined for the optimization process. By definition, depths shallower than the threshold depth are not relevant to whether or not the diver contracts DCS so they should not be used to calculate the parameters for dives above the threshold. Therefore, to prepare a model to be used to estimate risks for dives deeper than the threshold, we deleted 406 dives that were shallower than an estimated threshold of 20.5 fswg and simply fit the smaller dataset of 180 dives with Equation 1, without any other manipulation.

We were helped in settling on the 20.5 fswg threshold depth by a special approach: we assumed that any depth in the entire 586-dive dataset that is shallower than the threshold depth has the same effect as the threshold depth, so we commanded the computer program to reset all depths or equivalent-air depths less than a tentative *Thr* to be equal to the tentative *Thr*. Then to locate the *Thr* value that gave the highest negative log likelihood (*LL*) we repeatedly analyzed the data with Equation 1 using various tentative fixed values of *Thr*. The highest *LL* was observed with a *Thr* of 20.5 fswg. This procedure gave values for the threshold, D_{50}, exponent n, and *LL* that were nearly identical to those obtained when the below-threshold dives were deleted, but gave smaller asymptotic standard errors (ASE) and confidence intervals for the estimated *Pdcs* because it had the effect of adding 406 dives at depth of 20.5 fswg to the 180 above-threshold dives.

To develop models for evaluating the validity of the threshold concept, we fit the entire 586-dive dataset to two variants of Equation 1. In one, we fixed the *Thr* value at 20.5 fswg and set all depths below 20.5 equal to 20.5. In the other, we eliminated the threshold by fixing the *Thr* value at zero.

Details of the calculations.

The NONLIN module of SYSTAT provides an option, the *LOSS*, for constructing an error statement that differs from the least-squared-errors statement that is often used in statistics. Equation 2 is the *LOSS* statement we use; it is in terms of a single dive-outcome data point:

2) LOSS = - DIVES · (DCS · ln (ESTIMATE) + (1 – DCS) · ln (1 - ESTIMATE))

In Equation 2, *DIVES* is the number of divers in the group that makes up one of the 111 rows in the calibration dataset, where a row is a listing for one or more divers who followed the same profile and had the same outcome (DCS or no DCS). In the equation, *ln* signifies natural logarithms, and *ESTIMATE* is the estimated *Pdcs*. The *DCS* variable is either a one or a zero. Divers who followed the same profile and who did not contract DCS are listed together in the same row in the calibration dataset (*DCS* = 0, *DIVES* = 1 to 188), so *DIVES* multiplied by *(1 – DCS)* is simply the number of subjects in the row without DCS. Any diver who contracted DCS is listed in a separate row (*DCS* = 1, *DIVES* = 1). The *LOSS* function is the sum of *LOSS* statements given by Equation 2 over the entire calibration dataset.

To start estimating parameters, the SYSTAT program calculates an initial *Pdcs* for the first row of the calibration dataset from tentative, user-generated starting values of the parameters. Next the *LOSS* value is calculated from that *Pdcs* by Equation 2. The procedure is repeated for all rows and the *LOSS* is summed over all rows. The summed *LOSS* is recalculated to find a minimum by a quasi-Newton iteration process, which uses the first and second derivatives of the *LOSS* function to find new tentative parameter values. The iterations continue until differences between successive tentative parameter estimates reach predetermined small values. The minimized positive *LOSS* function (the sum of all *LOSS* statements by Equation 2) is the same as a maximized *LL* for maximum likelihood estimation of parameters. In addition to parameter estimation, the NONLIN module computes asymptotic standard errors (ASE) and the asymptotic correlation matrix of parameters by estimating the Hessian (second derivative) matrix after iterations have stopped. Note that the estimation process uses the individual dive-outcome results as they appear in the rows in the calibration dataset, not the data points that we generated for illustration purposes in Figure 1C by grouping dives together.

Three kinds of 95% confidence intervals are of interest. 1) We use the binomial theorem to calculate confidence intervals for the "true" incidence of DCS in a particular population from a limited sample of dives. 2) The NONLIN module calculates confidence intervals for estimated parameters. 3) We use the equations described by Ku (12) to calculate confidence intervals for the estimated probability of DCS from results of the statistical analysis (parameters, asymptotic standard errors, and correlation matrix); with these equations, the *Pdcs* and confidence intervals can be tabulated for the depth of each data point in the calibration dataset or for entries in a set of decompression instructions.

RESULTS

The top one-third of Table 2 shows particulars of the Thr20.5 Model, generated by fitting the 180 above-threshold dives to the Hill function given by Equation 1. The *LL* is much better than the *LL* for the null model. The lower two thirds of Table 2 show the two models based on the entire dataset. The *n* and D_{50} parameters are essentially the same for the Thr20.5 Model (top of Table 2) and the Thr20.5(ThrFixed) Model (middle of Table 2). The *n* exponent for the ThrZero Model (lowest) is six-fold larger

than the *n* for either of the Thr20.5 Models and far outside their confidence intervals, but the D_{50} values of the models are close to each other. The *LL* values of models based on the entire dataset, –54.90 vs. –57.66, indicates that the Thr20.5(ThrFixed) Model is superior to the ThrZero Model at the 95% confidence level according to a likelihood ratio test.

Table 3 shows probability estimates from two models. We estimated confidence intervals for the Thr20.5 Model in column 3 by the Ku equations (12) using the threshold model (top of Table 2) based on the 180-dive dataset. The confidence intervals are twice the *Pdcs* at 22 fswg and a little less than the *Pdcs* for 33-fswg exposures. The dashed box in Table 3 outlines where *Pdcs* estimated by the ThrZero Model is less than *Pdcs* by the Thr20.5 Model; *Pdcs* by the ThrZero Model is about half that by the Thr20.5 Model at 24 and 25 fswg. The ThrZero estimates are within the 95% confidence intervals for the Thr20.5 Model for depths shallower than 36 fswg.

Figure 2A shows complete dose-response curves; the 95% confidence intervals are very broad for the Thr20.5 Model at the right of the figure. The divergence of the ThrZero and Thr20.5 curves shows that extrapolation beyond the observed data can give very different predictions, depending on whether or not a model accounts for a threshold; for most of Figure 2A, the ThrZero curve is far above the Thr20.5 curve.

Figure 2B shows the region where the data points lie; the curve for the Thr20.5 model, generated from only 180 dives, follows the observed incidence points derived from the groups shown in the left-hand column of Table 1, but the ThrZero Model, generated from 586 dives, predicts lower incidence than is observed between 22 and 30 fswg and higher incidence than is observed to the right of 30 fswg. Figure 2C shows that the ThrZero Model predicts incidence that is well above the observed incidence for depths between 18 and 20 fswg.

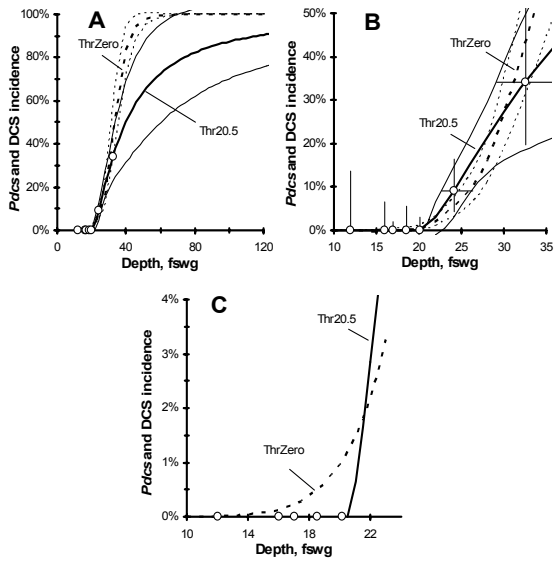

Fig. 2. Dose-response curves for human diving. A: the Thr20.5 and ThrZero Models; circles are the observed-incidence points from Figure 1C; light traces show 95% confidence intervals for the *Pdcs* estimates calculated by the Ku equations (12). B: panel A rescaled to emphasize the data points; vertical line segments show binomial 95% confidence intervals around the observed incidence points; horizontal line segments show one standard deviation on each side of the average depths. C: rescaled and simplified to show that the ThrZero Model predicts higher incidence than is observed in the low *Pdcs* range.

Chi-square analyses of the two models with fixed thresholds show that both models fit the data well and neither is preferable. We sorted the entire dataset by depth, bottom time, or predicted incidence and then apportioned the dives into bins containing approximately equal numbers of dives. Chi-square values of the contents of the resulting bins tend to be smaller for the Thr20.5 Model than for the ThrZero Model, but the differences between observations and model predictions could be due to chance at the 95% confidence level for both models.

TABLE 2. PARAMETERS, MODELS WITH AND WITHOUT THRESHOLDS

Thr20.5 Model: *LL* = -54.90, 180 dives, null model LL = -66.84

Parameter	Estimate	ASE*	Param/ASE	95% Conf. Interval
Thr	20.49897	0.220848	92.82	20.06 – 20.94
n	1.381602	0.435966	3.17	0.509 - 2.255
D_{50}	39.792747	7.164622	5.55	25.45 - 54.14

Correlation matrix

	Thr	*n*	D_{50}
n	1.0000		
n	-0.209761	1.0000	
D_{50}	0.111538	-0.882043	1.0000

Thr20.5 Model (Fixed Thr), *LL* = -54.90, 586 dives, null model LL = -93.80

Parameter	Estimate	ASE*	Param/ASE	95% Confidence Interval
Thr	20.5 (fixed)			
n	1.381199	0.333775	4.14	0.718 - 2.044
D_{50}	39.796173	5.578312	7.13	28.72 - 50.87

Correlation matrix

	n	D_{50}
n	1.0000	
D_{50}	-0.8879	1.0000

ThrZero Model, *LL* = -57.66, 586 dives, null model *LL* = -93.80

Parameter	Estimate	ASE*	Param/ASE	95% Conf. Interval
Thr	zero (fixed)			
n	8.936685	1.055800	8.46	6.84 - 11.03
D_{50}	33.628133	1.104747	30.44	31.43 - 35.82

Correlation matrix

	n	D_{50}
n	1.0000	
D_{50}	-0.736374	1.0000

* ASE = asymptotic standard error

TABLE 3. PROBABILITY OF DCS FOR NO-STOP ASCENTS FROM SATURATION DIVES (HUMAN)

Values for dives deeper than 33 fswg are extrapolations from shallower depths.

(1) Depth, fswg	(2) ***Thr20.5* Model**	(3) 95% confidence interval	(4) ***ThrZero* Model**
12	0.0%	--	0.0%
16	0.0%	--	0.1%
20	0.0%	--	0.9%
21	0.1%	-0.4% - 1.6%	1.5%
22	2.9%	-0.9% - 6.6%	2.2%
23	5.6%	0.5% - 10.7%	3.2%
24	8.6%	2.9% - 14.4	4.7%
25	12%	6% - 18%	6.6%
26	15%	8 - 22%	9%
27	18%	11 - 25%	12%
28	21%	13 - 30%	16%
29	24%	15 - 34%	21%
30	27%	16 - 38%	26%
31	30%	17 - 43%	33%
32	33%	18 - 48%	39%
33	35%	19 - 52%	46%
34	38%	20 - 56%	53%
35	40%	21 - 60%	59%
36	42%	21 - 64%	65%*
37	45%	22 - 67%	70%*
38	47%	23 - 70%	75%*
39	49%	24 - 73%	79%*
40	50%	24 - 76%	83%*

* = values above the 95% confidence interval for the *Thr20.5 Model*

DISCUSSION

Our calibration dataset provides strong evidence of a threshold in humans subjected to direct ascent from saturation air dives (Figure 1C). Figure 3A shows that there is also a threshold in swine. Confidence intervals for most of the points in Figure 3A are large because the number of animals is small, except for the point at 110 fswg, which represents 44 animals with 30 DCS cases (13). The threshold for these 20-Kg swine is at 80 fswg, in contrast to 20.5 fswg for our human data. There were 564 DCS-free dives for the human data shown in Figure 1C, but there are only 47 DCS-free swine. We grouped 18 DCS-free swine together to get the confidence interval that is farthest to the left on the figure.

There are data points in the range of 50% to 100% DCS incidence in Figure 3A, whereas the human data in Figure 1C reaches only to 34%. The positions of the curves in Figure 3A are determined by the location of the bulk of the data, so the threshold and no-threshold curves are near each other at depths near 100 fswg. The curve with threshold (D_{50} = 95.1 fswg, *n* =

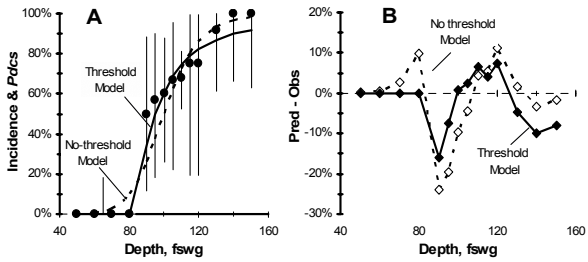

Fig. 3. Occurrence of DCS in 128 young swine (20 Kg) that were subjected to direct ascent from air saturation dives, drawn from Table 1 in the publication of Dromsky et al. (13). A: two Hill-function fits to the data points, one with and one without a threshold; vertical line segments are binomial 95% confidence intervals around the observed-incidence points. B: differences between the incidences predicted by two models and the observed DCS incidences.

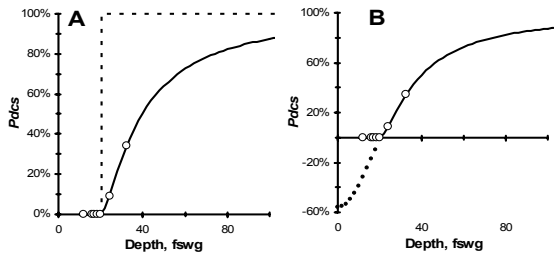

Fig. 4. Types of threshold. A: a step phenomenon or all-or-none threshold (dashed) compared with the curve for the Thr20.5 Model, in which a probabilistic phenomenon is cut off at the left end; circles are data points seen first in Figure 1C. B: we speculate that the probabilistic phenomenon extends to depths shallower than the threshold, but no longer has any effect.

1.59, LL = 57.67) is near the data points in the 50% to 80% *Pdcs* range but the three highest points are near the curve without threshold (D_{50} = 99.89 fswg, n = 10.0, LL = 59.19). The predictions by the no-threshold swine model are above the observed points at shallow depths and below them for intermediate-depth dives (Figure 3B). A likelihood ratio test indicates that the Threshold Model fits the data better than the No-Threshold Model at the 90% confidence level, but not at the 95% level.

Threshold as a discontinuity.

Sometimes a threshold is thought of in all-or-none terms. According to the dashed all-or-none threshold in Figure 4A, a saturated diver would be free of DCS if he made a direct ascent from a depth that is to the left of the vertical line segment and would be certain to have DCS if the depth were to the right of the vertical. This kind of threshold is not compatible with the datasets we used for no-stop ascents from saturation by humans and swine. Instead, the solid curve in Figure 4A illustrates how, for dives deeper than the threshold depth, a diver is subject to rising probability of DCS as the depth increases. A continuous process is interrupted at 20.5 fswg; we speculate that the process gives an S-shaped curve that continues at shallower depths (dotted trace in Figure 4B) but does not produce DCS.

We can estimate the critical drop in absolute pressure that would give rise to DCS in human divers who make direct ascents from air-breathing saturation dives. A diver who is saturated at 20.5 fswg, the threshold depth for limb bends, would be under pressure of 1.62 atmospheres absolute (1 atm plus 20.5 fswg/33 fswg). After direct ascent to the surface, the pressure is 1.0 atm. A pressure ratio greater than 1.62/1 would cause damaging bubbles and the greater the ratio, the higher the DCS incidence.

A plausible explanation for the discontinuous nature of the threshold can be made by invoking the idea that the bubbles that cause DCS are generated from stabilized gaseous micronuclei that reside in the body at unknown sites (14,15). According to some theories about gaseous micronuclei, physical force due to a surrounding structure constrains the gas in micronuclei. When a change of pressure during a decompression causes bubbles to form, it is presumably because the pressure change on the gas inside the micronucleus is great enough to cause the structure itself to become ineffective so that the gas inside is freed to become bubbles, or to cause damaging bubbles to bud off from the gas inside the

micronucleus. Because venous gas emboli are observed at milder decompressions than those that cause DCS, we speculate that venous gas emboli are generated from a different population of micronuclei than those that cause DCS.

Implications for operational diving.

There is considerable uncertainty in our estimates. Confidence intervals are large because of the limited number of dives and DCS cases in the calibration dataset. We believe that models that are generated from low-incidence data only and do not account for thresholds are suspect, based on the evidence for thresholds in humans in Figure 1C and swine in Figure 3. We recommend the estimates given by the Thr20.5 Model in column 2 of Table 3 for operational saturation dives shallower than 33 fswg. For example, column 2 shows that risk of DCS is zero at 20 fswg and 2.9% at 22 fswg. At 30 fswg the risk is 27% and the 95% confidence interval is large -- 16% to 38%.

Lack of data prevents us from making recommendations about depths deeper than 33 fswg. The deepest dive in our dataset is at 38 fswg, a DCS case (last line of Table 1; the *Pdcs* estimate by the Thr20.5 Model is 46%). To probe the impact of high-risk dives on a dose-response curve, we arbitrarily added 13 false DCS cases at 60 fswg to our human dataset. The added dives had a major effect on the slope and position of the dose-response curve – the resulting dose-response curve (not shown) was shifted up so that it was near the trace for the ThrZero Model and had a threshold of 17.5 fswg.

Some investigators have attempted to improve direct-ascent *Pdcs* predictions for dangerous dives by adding high-incidence animal data to the available low-incidence human data (4,5). However, such mixing of species adds to uncertainty because of the required assumptions about how the animal data should be re-scaled so that it fits with human data. When we arbitrarily shifted each of the depths of the swine data points to the left by subtracting 59.5 fswg so that the dose-response curves of the humans and swine superimposed at a common threshold, the shifted swine DCS-incidence points described a curve that was a little steeper than the human Thr20.5 Model curve and therefore higher than it, but not as high as the ThrZero Model curve. We doubt that this is helpful for predicting human DCS – we do not know whether the D_{50} and n parameters in swine models should also be altered when used to augment human data.

ACKNOWLEDGEMENT

This work was supported in part by the Deep Submergence Biomedical Development Program, Naval Sea Systems Command, Program Element 0603713N, Project S0099. The opinions and assertions contained herein are the private ones of the authors and are not to be construed as official or as reflecting the views of the Naval Sea Systems Command or the U.S. Navy.

REFERENCES

1. Parker EC, Ball R, Tibbles PM, Weathersby PK. Escape from a disabled submarine: decompression sickness risk estimation. *Aviat Space Environ Med* 2000; 71: 109-114.
2. Bell PY, Harrison JR, Page K, Summerfield M. An effect of CO_2 on the maximum safe direct decompression to 1 bar from oxygen-nitrogen saturation. *Undersea Biomed Res* 1986; 13:443-455.
3. *U.S. Navy Diving Manual. Revision 4.* Publication SS521-AG-PRO-010. Naval Sea Systems Command. Washington DC, 1999.
4. Lillo RS, Himm JF, Weathersby PK, Temple DJ, Gault KA, Dromsky DM. Using animal data to improve prediction of human decompression risk following air-saturation dives. *J Appl Physiol* 2002; 93: 216-226.
5. Ball R, Lehner CE, Parker EC. Predicting risk of decompression sickness in humans from outcomes in sheep. *J Appl Physiol* 1999; 86:1920-1929.
6. Weathersby PK, Homer LD, Flynn ET. On the likelihood of decompression sickness. *J Appl Physiol* 1984; 57: 815-824.
7. Parker EC, Survanshi SS, Massell PB, Weathersby PK. Probabilistic models of the role of oxygen in

human decompression sickness. *J Appl Physiol* 1998; 84: 1096-1102.
8. Temple DJ, Ball R, Weathersby PK, Parker EC, Survanshi SS. The dive profiles and manifestations of decompression sickness cases after air and nitrogen-oxygen dives. *NMRC Technical Report 99-02,* Naval Medical Research Center, Bethesda MD, May 1999.
9. Weathersby PK, Survanshi SS, Nishi RY, Thalmann ED. Statistically based decompression tables VII: Selection and treatment of primary air and N_2O_2 data. *Joint Technical Report, NSMRL #1182 and NMRI 92-85*, Naval Medical Research Institute, Bethesda MD, Sept 1992.
10. Eckenhoff RG, Olstad CS, Carrod G. Human dose-response relationship for decompression and endogenous bubble formation. *J Appl Physiol* 1990; 69: 914-918.
11. Eckenhoff RG, Osborne SF, Parker JW, Bondi KR. Direct ascent from shallow air saturation exposures. *Undersea Biomed Res* 1986; 13: 305-316.
12. Ku HH. Notes on the use of propagation of error formulas. *J Res Natl Bur Stand Eng Instr* 1966; 70C: 263-273.
13. Dromsky DM, Toner CB, Survanshi S, Fahlman A, Parker E, Weathersby PK. Natural history of severe decompression sickness after rapid ascent from air saturation in a porcine model. *J Appl Physiol* 2000; 89:791-798.
14. Yount DE and Strauss RH. Bubble formation in gelatin: a model for decompression sickness. *J Appl Physics* 1976; 47: 5081-5089.
15. Van Liew HD, Raychaudhuri S. Stabilized bubbles in the body: pressure-radius relationships and the limits to stabilization. *J Appl Physiol* 1997;82:2045-2053.